Ocean Science Journal, Vol. 41 No. 3, 149-161(2006)

Article

Ocean Science Journal

http://osj.kordi.re.kr

Relationship between Mn Nodule Abundance and Other Geological Factors in the Northeastern Pacific: Application of GIS and Probability Method

Youngtak Ko[1]*, Saro Lee[2], Jonguk Kim[1], Ki-Hyune Kim[1], and Mee-Sook Jung[1]

[1]*Marine Resources Research Department, KORDI, Ansan P.O. Box 29, Seoul 425-600, Korea*

[2]*Geoscience Information Center, Korea Institute of Geoscience & Mineral Resources, Daejeon 305-350, Korea*

Received 23 August 2006; Revised 6 September 2006; Accepted 26 September 2006

Abstract – The aims of this study are 1) to construct a database using geostatistics and Geographic Information System (GIS), and 2) to derive the spatial relationships between manganese nodule abundance and other geological factors such as metal grade, slope, water depth, topography, and acoustic characteristics of the sub-bottom. Using GIS, it is possible to analyze a large amount of data efficiently, and to maximize the practical application, to increase specialization, and to enhance the accuracy of the analyses. The greater the copper and nickel grade, the higher the rating. The distribution pattern of nickel grade is similar to that of copper grade. The slopes are generally less than 3° except for seamounts and cliff areas. The rating shows no correlation with slope. The rating is highest for slopes between 2.5 and 3.5° in block N1 and between 4.0 and 4.5° in block N3. The topography is classified into five groups: seamount, hill crest, hill slant, hill base or plain, and seafloor basin or valley. The rating proves lowest for seamount and hill crest. Our results show that the rating increases with the water depth in the study area. Nodule abundance dose not show any significant relationship with the thickness of the upper transparent layer in the study area.

Key words – Manganese nodule, GIS, spatial relationships, rating, northeastern Pacific

1. Introduction

Submarine ferromanganese concretion was first discovered in the Kara Sea of Russia in 1868 (Earney 1990). In the course of its round-the-world expedition from 1873 to 1876, HMS Challenger collected many small dark-brown balls, rich in manganese and iron, which were named manganese nodules (Manheim 1978; Earney 1990). Since the 1960s, manganese nodules have been recognized as a potential source of nickel, copper, cobalt, and manganese, especially considering the progressive depletion of land-based mineral resources. Manganese nodules are found on the seabed in many areas, and have been comparatively well-studied for their distribution because of their potential economic importance. These nodules are most abundant in the Clarion-Clipperton Fracture Zone (C-C zone). And thus, the C-C zone has been the focus of much international attention (Mero 1965; Frazer 1979; McKelvey *et al.* 1979; Bernhard and Blissenbach 1988).

The ultimate purpose of the study of manganese nodules is to find out nodule deposits that are economically feasible for commercial development. The selection of manganese nodule deposits has been determined by geological and economic criteria provided by specialists. France fixed the criteria for manganese nodule deposits in terms of nodule abundance (> 5 kg/m^2), metal grade (Cu+Ni > 2.5%), slope of the seabed (< 10°), spatial continuity of nodule deposits (the absence of nodules < 1,000 m), and the height of the escarpment (< 1 m) (IFREMER 1989). Korea also set criteria similar to France, but more specific cutoff grades for Cu (> 1.03% or 50 g/m^2) and Ni (1.24% or 60 g/m^2) (MOMAF 1997, 1999).

Recently, a geographic information system (GIS) was adopted to deep-sea resources data such as manganese nodules or crusts with advances in computer technology. Using GIS, it is possible to analyze large amounts of data with increased efficiency, and to maximize the management of

*Corresponding author. E-mail: ytko@kordi.re.kr

practical applications. The use of probability and statistical methods allows for more specialized studies and enhances the accuracy of the analysis. For these advantages, GIS and probability methods were used for suitable site investigation of manganese nodules. However, the use of GIS in the deep-sea resource field has been limited by the construction of database (JICA and MMAJ 2000) or a qualitative decision for rating and weighting of previous study on a partial block of the Korean allocated area (Ko 1997).

The objectives of this study are (1) to construct a database using geostatistics and GIS, and (2) to derive the spatial relationships between nodule abundance and other geological factors such as metal grade, slope, water depth, topography, and acoustic characteristics of the sub-bottom. The probability and statistical methods were newly adopted to the study area. The rating was quantified by applying probability methods to a database and to development potential maps produced by GIS.

2. Materials and Methods

The study area is located in the central part of the C-C zone, between 16° and 17°N latitude, and 125° and 134°W longitude, in northeastern Pacific (Fig. 1). The study area is composed of two blocks, N1 and N3, which is the area designated for Korea. The water depth of the study area ranges from 3,682 m to 5,485 m. The depth is generally greater than 4,800 m, and slopes gently toward the northwest. The seafloor is older toward the northwest and is largely offset by a fracture zone which is indistinct in the general bathymetric trend. Several seamounts of various sizes are aligned in an E-W trend. They form ridges, which is the general bathymetric pattern in the C-C zone. Most seamounts

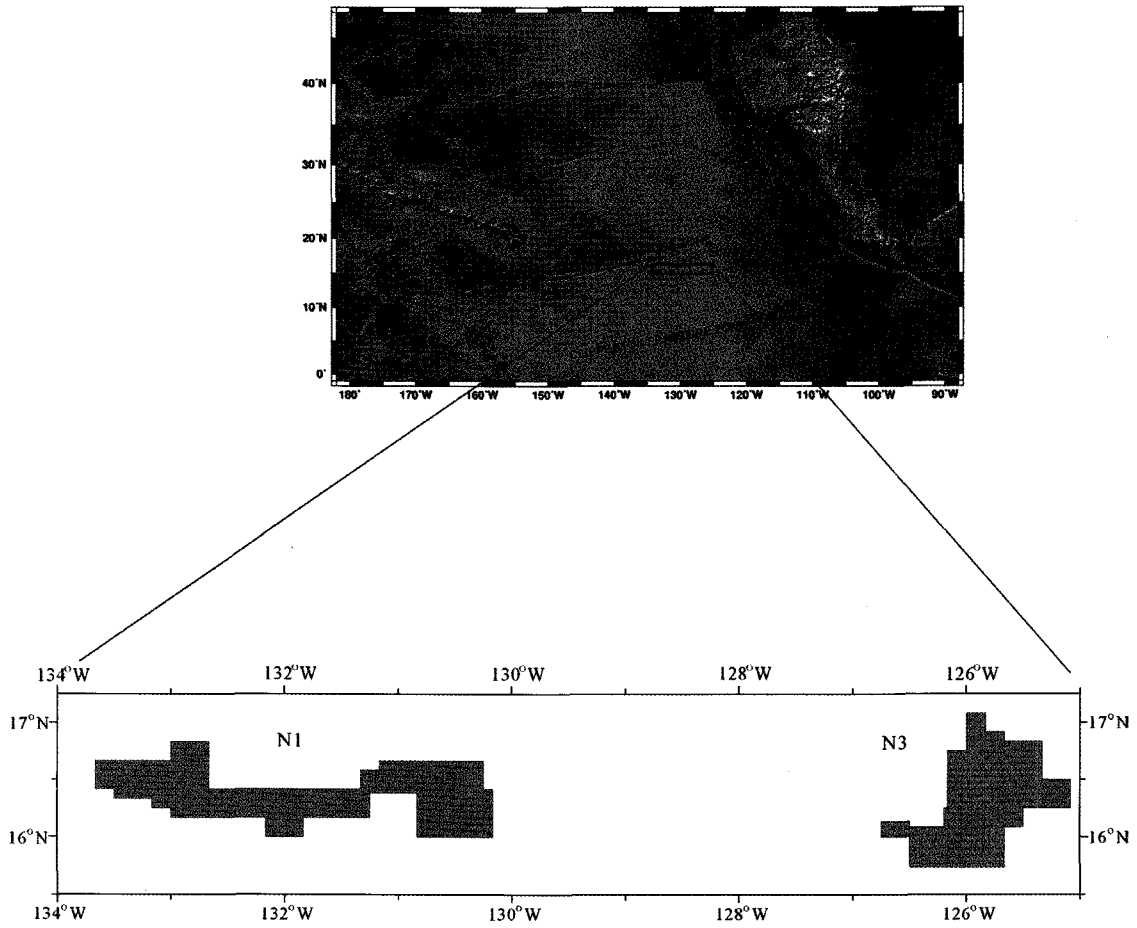

Fig. 1. Location of study area in the northeastern equatorial Pacific. It is located in the central part of the C-C zone, between 16° and 17°N latitude, and 125° and 134°W longitude, in northeastern Pacific. The study area is composed of two blocks, N1 and N3, which is the area designated for Korea.

lack sediments on the tops and slopes, some seamounts are covered with a thick sediment layer and are complicated with irregular block and step faults. The seafloor basement is also irregular.

Using the nodule abundance obtained from sampling data together with a spatial database, two analytical methods were applied. The rating was calculated by analyzing the correlation between nodule abundance and the metal grade, slope, water depth, topography, and acoustic characteristics of the sub-bottom. By combining GIS with probability methods, the relationships and contrast values between nodule abundance and each factor affecting abundance were assessed.

Manganese nodule abundance

Sampling and abundance measurement of manganese nodules were performed to understand their distribution pattern in the study area and to obtain the basic data for estimation and evaluation of metal grade using geostatistical methods. The nodules were sampled from 187 stations in N1 block and 139 stations in N3 block, respectively. These nodules are formed at the sediment and water interface and show various properties in surface texture, morphology and size. Most nodules collected in N1 and N3 blocks show smooth to transitional surface texture and occur as spheroid or poly nodule shapes, which might be due to relatively rough topography in the studied area by several seamounts. The nodule abundance was determined by collecting nodules from a small area of the seafloor using a Free Fall Grab (FFG). Photographs of the seafloor obtained by a camera attached to the FFG were used to correct nodule abundance estimated from the nodule samples collected by FFG.

The nodule abundance was defined as the nodule weight collected by the FFG per unit area (kg/m^2), which can be expressed by the following equation:

$$Ab. = \frac{Wi}{S} \quad (1)$$

where *Ab.* is the nodule abundance (kg/m^2), *Wi* is the weight of collected nodules (kg) and *S* is the collection area of FFG (m^2)

The collected abundance of manganese nodules should be subjected to revision before applying it to an estimation of the nodules' population and abundance, because the collected nodule amount is lower due to a collection efficiency of grabs of less than 1. The abundance of manganese nodules (*Ab.*) was corrected by multiplying the correction constant of 1.29 (MOMAF 1996) which was determined from the comparison with photo data acquired from past cruises. The correction constant of 1.29 is similar to the value which was suggested by the experimental method of the Ocean Minerals Company (OMCO 1992).

$$Y = 1.29 \times Ab. \quad (2)$$

where Y is the corrected abundance of Mn nodule, *Ab.* is the sample abundance and 1.29 is the correction constant.

The collected manganese nodules were analyzed for major and minor elemental concentrations using an Inductively Coupled Plasma Atomic Emission Spectrometer (ICP-AES). Sampling data include position, depth of the sampling site, abundance of nodules (in wet kg/m^2) and contents of manganese, nickel, copper, cobalt, and other metals in terms of the percentage of dry weight. The whole data are essential for analyzing the resource distribution in the seafloor. The data analyses for copper and nickel grade were carried out using GIS to find out the relationship between the metal grade and nodule abundance.

The grade of metals was obtained by multiplying manganese nodule abundance (kg/m^2) to metal content (%). The unit of the metal grade is defined by the weight per unit area (g/m^2). The cutoff grade of abundance was fixed at 5 kg/m^2. The cutoff grade of copper is 1.03% or 50 g/m^2, and the cutoff grade of nickel is 1.24% or 60 g/m^2 (Archer 1976; Holser 1976; Kildow *et al.* 1976; Frazer 1977; Park 1995).

The analyses for copper and nickel grade were carried out using Spatial Analyst and 3D Analyst module of ARC/INFO to determine the relationship between the metal grade and nodule abundance. The grade of copper and nickel is represented by a gram per unit area (g/m^2). It is classified into 18 and 23 groups at a 10 gram interval.

Multibeam echo sounding data

Swath bathymetric data were obtained to evaluate the geomorphic and topographical features of the study area using a SeaBeam 2000 and Sealogger system on board the R/V Onnuri. A SeaBeam 2000 has 121 beams and a swath width of 92 degree with a frequency band of 12 kHz. The propagation velocity of the sound underwater is affected by water temperature, and by the the physical

properties of a medium; these are important collection variables for the calculation of slope distance (Medwin and Clay 1997; Jones 1999). Sound velocity profiles were obtained for water depth using XBT (Expandable Bathythermograph) and CTD (Conductivity, Temperature, Dissolved Oxygen) data. Recorded multibeam swath data were processed using a MB-System software which was built on the GMT utilities. To remove noise, a built-in module in the MB-system 'mbedit' was applied to each ping.

Based on multibeam echo sounding data, slope analysis of the seafloor was carried out using a Spatial Analyst and 3D Analyst module of ARC/INFO to determine the relationship between slope and nodule abundance. Each sample point has an X, Y coordinate and Z-Value as a bathymetry. The study area shows slopes dominantly less than 5°. The slope was divided into a total of 23 groups: 0.5° interval for the range of 0° to 5°, 1° interval for the range of 5° to 10°, 2° interval for the range of 10° to 20°, 5° interval for the range of 20° to 30°, and one group for the range of 30° to 90°.

Water depth analysis was carried out to determine the relationship between water depth and nodule abundance. It is classified into 21 groups at a 100 m depth interval.

Topography analysis was carried out to establish the relationship between the topography of the seafloor and nodule abundance. It is classified into 5 groups such as seamount, hill crest, hill slant, hill base or plain, and seafloor basin or valley. It is difficult to classify topography, because the criterion for topographic classification is not defined clearly in the study area, but the following definitions were used for the classification of topography in this study. A mountain on the ocean floor which does not break the water surface was classified as a seamount, while a conically shaped mountain less than 1,000 m in height is an isolated steep-sided hill (Allaby and Allaby 1999). Abyssal hills are defined as relatively small topographic features developed in a predominantly flat, deep-ocean floor, commonly 50-250 m in height and a few km in width. They are the most common topographic features of the Pacific Ocean floor at depths of 3,000-6,000 m. The basin or seafloor basin represents a major relief depression, influenced by the structure, or formed by erosion. The plain is defined as a flat area, developed at a low elevation. It is an extensive region of comparatively smooth and level area with gently undulating land lacking prominent surface irregularities. The covering sediments are usually thin layers of a pelagic ooze or distal turbidite. The valley is defined as a wide, low relief depression of the ocean floor with gently sloping sides.

Sub-bottom profile data

A high frequency sub-bottom profile that penetrates up to several tens of meters below the seafloor is a useful tool in understanding the characteristics of sea bottom sediments without in-situ sampling, because characteristics of reflected echoes are controlled by texture and geometry of sediments (Damuth and Hayes 1977; Damuth 1978; Pratson and Laine 1989; Kuhn and Weber 1993; Chough *et al.* 1997; Dowdeswell *et al.* 1997; Taylor *et al.* 2000). Sediment layers are essential for nodule's growth by diagenesis and benthic activity (Stackelberg and Beiersdorf 1991; Jung and Lee 1999). The thickness of the sediment layer is related to the sedimentation rate, which in turn has a strong effect on the growth of manganese nodules. Generally, abundance of manganese nodules is high in a sediment-starved area and low where surface productivity and the carbonate sedimentation rate are high (Skornyakova and Murdmaa 1992). Thus, the formation of manganese nodules is dependent on the characteristics of the uppermost sediment layer, and the distribution of manganese nodules could be inferred from the nature of the uppermost sediment layer (Usui and Tanahashi 1992; Jeong *et al.* 1994, 1996).

Sub-bottom profiles are classified into three types of acoustic layers: an acoustically transparent layer (TL) lacking an internal reflection layer, an acoustically opaque layer (OL) produced from an acoustically perfect reflective layer, and an acoustically stratified layer (SL) with densely internal reflection layers (Kim *et al.* 1998). The acoustically transparent layer is from the uppermost sedimentary layer. The transparent layer is generally thick on the seafloor basin and valley, thin or non-existent in other areas. The abundance of manganese nodules is known to have an inverse relationship against the thickness on the acoustically transparent uppermost sedimentary layer in the Central Pacific and C-C zone (Usui and Tanahashi 1986; Jeong *et al.* 1994, 1996). An inverse relationship of nodule abundance to the thickness of uppermost sediment layer indicates that erosional processes facilitate nodule generation by bottom currents (Glasby 1978; Mizuno *et al.* 1980; Usui *et al.* 1987). The sediment composition of radiolarian ooze and clay, with high porosity and similar

density, is responsible for the acoustic transparency of the uppermost sediment layer.

The acoustically transparent layer, obtained by 3.5 kHz high-resolution seismic profiler, is useful for the study of manganese nodule distribution, sub-bottom sediment structure and distribution, and sedimentary sequence distribution to tens of meters (Usui and Tanahashi 1986; Usui *et al.* 1987). High-resolution (3.5 kHz) sub-bottom profiles were obtained at the manganese nodules' sampling sites using a Bathy-2000P using FM or chirp mode source. The subbottom profile data were obtained where FFGs were deployed and along the shifting line between these stations. Data in the sampling stations generally have better qualities than those on the shifting line, because the research vessel was moving slowly at these stations to recover FFG samples. In this study, the sub-bottom profile data was used for analysis of transparent layer distribution using the kriging method. The acoustic characteristics of near-surface sediments from a high-resolution sub-bottom profile on the sampling sites were analyzed to calculate the abundance of manganese nodules, especially in terms of the thickness of the upper transparent layers. Transparent layer thickness ranges from 0 m to 90 m.

Calculation relationships between manganese nodule abundance and geological factors

The database for factors related to manganese nodule development, such as manganese nodule abundance, metal grade from geochemical analysis, geomorphic characteristics, and acoustic characteristics, was constructed using GIS. Using the sampling data of manganese nodule abundance and the constructed spatial database, an analysis method was applied. A probability analysis was performed and the rating of each factor was calculated.

The calculated and extracted factors were converted into a 100×100 m grid using the GIS, and then converted into Data Base File (DBF) data in order to determine statistical relationships between the sampling abundance and each factor, such as the copper and nickel grade, slope, water depth, topography, and transparent layer thickness. The rating was calculated by analyzing the correlation between nodule abundance and the metal grade, slope, water depth, topography, and acoustic characteristics of the sub-bottom such as that given in equation (3):

$$R = \frac{\sum w \times Np}{Nt} \quad (3)$$

where R is the rating of each class, w is the weight of the sampling abundance, Np is the number of the sampling point and Nt is the total number of the sampling points

3. Results

Relationship between copper grade and manganese nodule abundance

In block N1, the copper grade ranges from 4.2 to 141.1 g/m^2 unit with an average of 44.6 ± 22.0 g/m^2 (average ± 1 s.d.) (Fig. 2a). The area containing the nodule with the copper grade of over 50 g/m^2 covered 33% of the block. Overall, the greater the copper grade, the higher the rating. A rich zone occurs in the west along the NWW-SEE axis, with impoverished zones occupying a NE-SW zone in the western and central parts of the block. Much of the area of this block has a low copper content (Fig. 3a).

In block N3, the copper grade ranges from 3.1 to 150.3 g/m^2 unit with an average 46.1±20.8 g/m^2 (Fig. 4a). The area containing the nodule with the copper grade of over 50 g/m^2 covered 34% of the block. The regression equation obtained using probability methods gives $Y = 0.62X - 3.36$, $R^2 = 0.29$. The reduction of slope and R^2 arises from an anomalous datum that exists in class 150-160. Overall, the greater the copper grade, the higher the rating. There is a rich circular zone in the southwest, with an impoverished zone in the northern part of the block (Fig. 5a).

Relationship between nickel grade and manganese nodule abundance

The distribution pattern of nickel grade is similar to that of copper grade. In block N1, the nickel grade ranges from 5.8 to 175.6 g/m^2 unit with an average of 60.6 ± 26.4 g/m^2 (Fig. 2b). The area containing the nodule with the nickel grade of over 60 g/m^2 covers 46% of the block. Over 69% of the area was between 30 and 80 g/m^2. Sampling stations are distributed over 67% of the block at ranges from 20 to 70 g/m^2. In general, the greater the nickel grade, the higher the rating. The distribution pattern is similar to that for copper (Fig. 3b). The regression equation obtained using probability methods gives $Y = 0.99X + 0.16$, $R^2 = 0.91$.

In block N3, the nickel grade ranges from 4.7 to 182.6

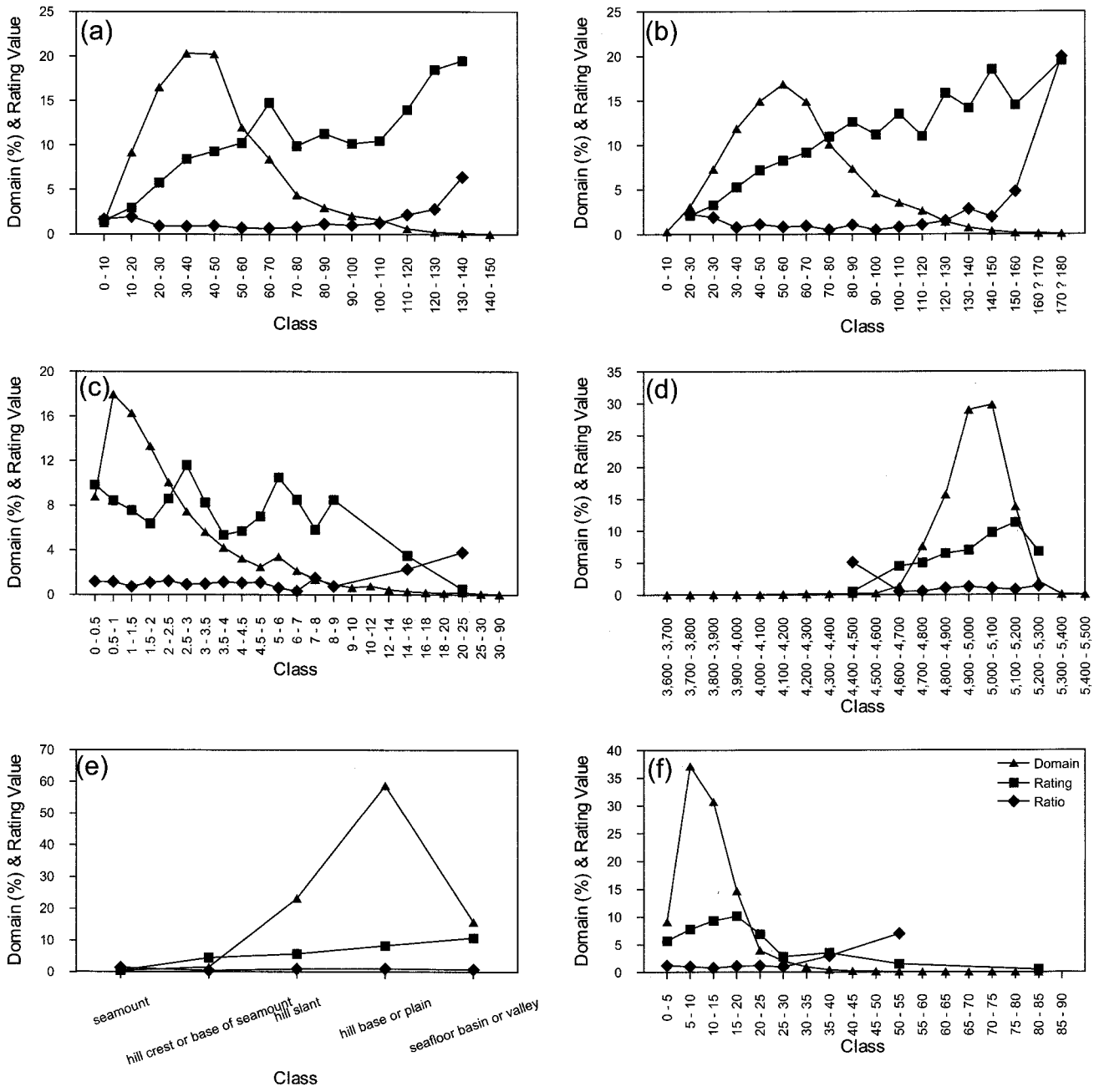

Fig. 2. The relationship between (a) domain and copper grade, rating and copper content, (b) domain and nickel content, rating and nickel grade, (c) domain and slope, rating and slope, (d) domain and water depth, rating and water depth, (e) domain and topography, rating and topography, (f) domain and transparent layer thickness, rating and transparent layer thickness, for block N1.

g/m^2 unit with an average of 63.8 ± 25.7 g/m^2 (Fig. 4b). The zone containing the nodule with the nickel grade of over 60 g/m^2 covers 51% of the block. Over 64% of the area is between 40 and 80 g/m^2. Sampling stations are distributed over 66% of the block at ranges from 20 to 70 g/m^2. In general, the greater the nickel grade, the higher the rating. The distribution pattern is similar to that for copper (Fig. 5b). The regression equation obtained using probability methods gives $Y = 0.86\ X + 0.89$, $R^2 = 0.90$.

Relationship between slope and manganese nodule abundance

In general, the slope is less than 3°, except for seamounts and cliff areas. It is difficult to make a precise correlation

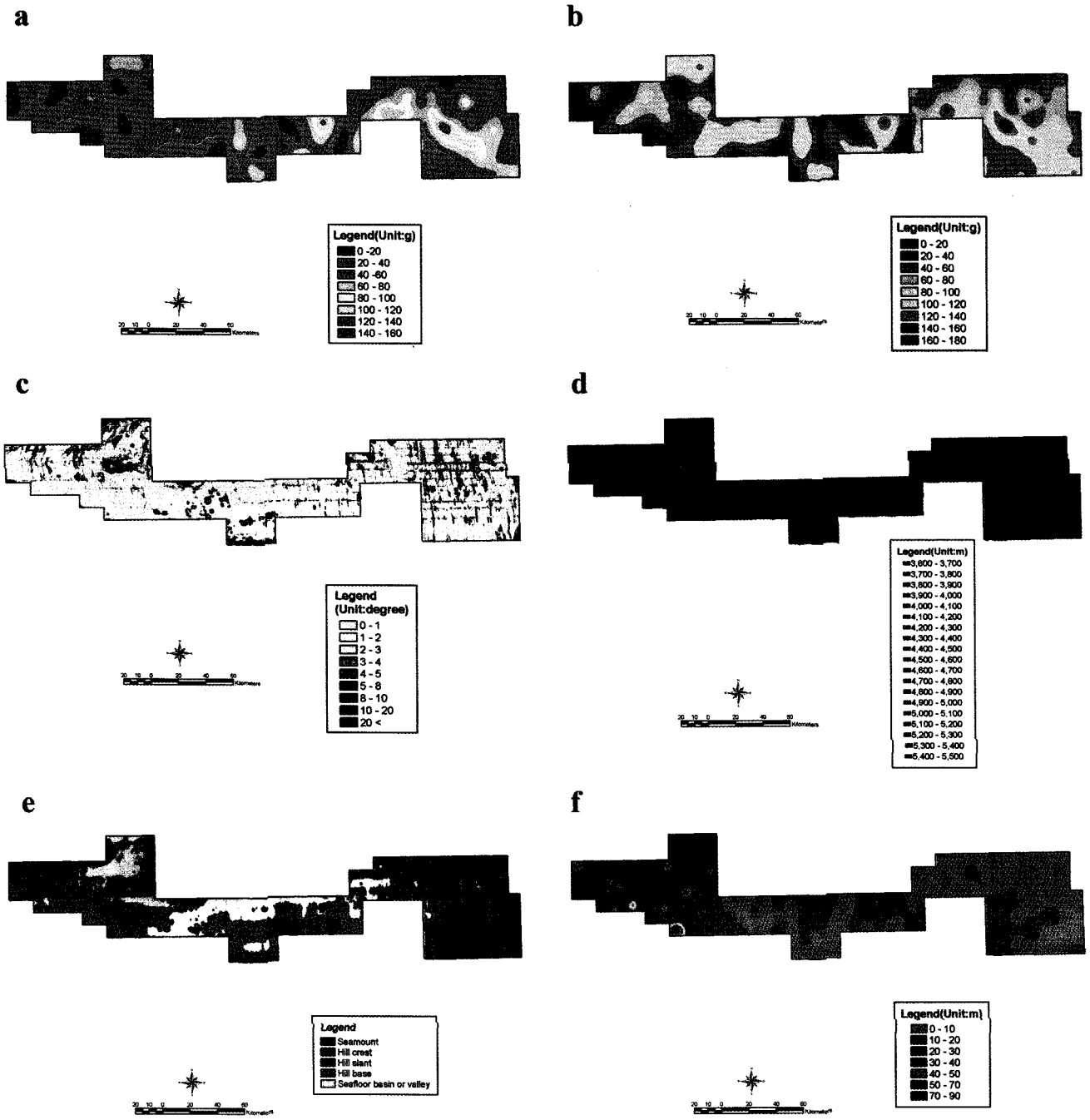

Fig. 3. The distribution map of (a) copper grade, (b) nickel grade, (c) slope, (d) bathymetry, (e) topography, (f) transparent layer thickness, for block N1.

between slope and nodule abundance. In block N1, Slope ranges from 0 to 44° with an average of 2.5 ± 2.6° and is classified into 23 groups (Fig. 2c). The area occupied by slopes below 5° is 89%. Sampling stations are distributed such that 87% lay in areas with slopes from 0 to 4°. Rating is highest in class 0-1° and 2.5-3.5°. The seamount areas in the central-western part of the block and at the base of the central part have steep slopes (Fig. 3c).

In block N3, slope ranges from 0 to 34.5° with an average of 1.8 ± 1.7° and is classified into 23 groups (Fig. 4c). 96% of the whole area is occupied by slope below

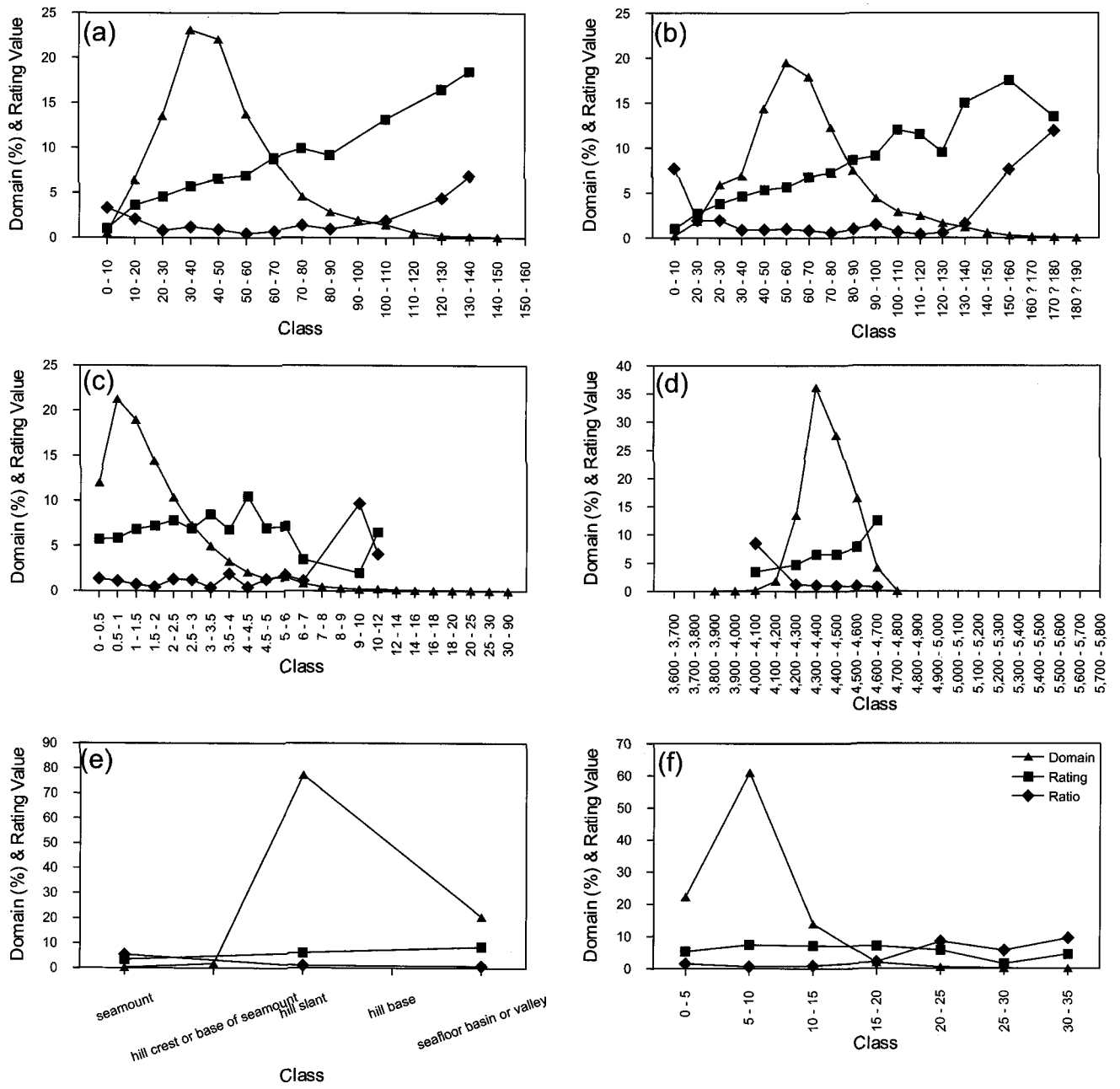

Fig. 4. The relationship between (a) domain and copper grade, rating and copper content, (b) domain and nickel content, rating and nickel grade, (c) domain and slope, rating and slope, (d) domain and water depth, rating and water depth, (e) domain and topography, rating and topography, (f) domain and transparent layer thickness, rating and transparent layer thickness, for block N3.

5°. Sampling stations are distributed such that 83% lie in areas with slope from 0 to 3°. Rating is highest in class 1.5 - 3.5° and 4 - 6°. In general, the greater the slope, the lower the rating. The seamount areas in the central and upper parts of the block have the steepest slopes (Fig. 5c).

Relationship between water depth and manganese nodule abundance

The rating increased with increasing water depth in the study area. In block N1, the water depth ranges from 3,632 to 5,485 m with an average of 4,974 ± 131.7 m. Water depth in block N1 is classified into 19 groups (Fig.

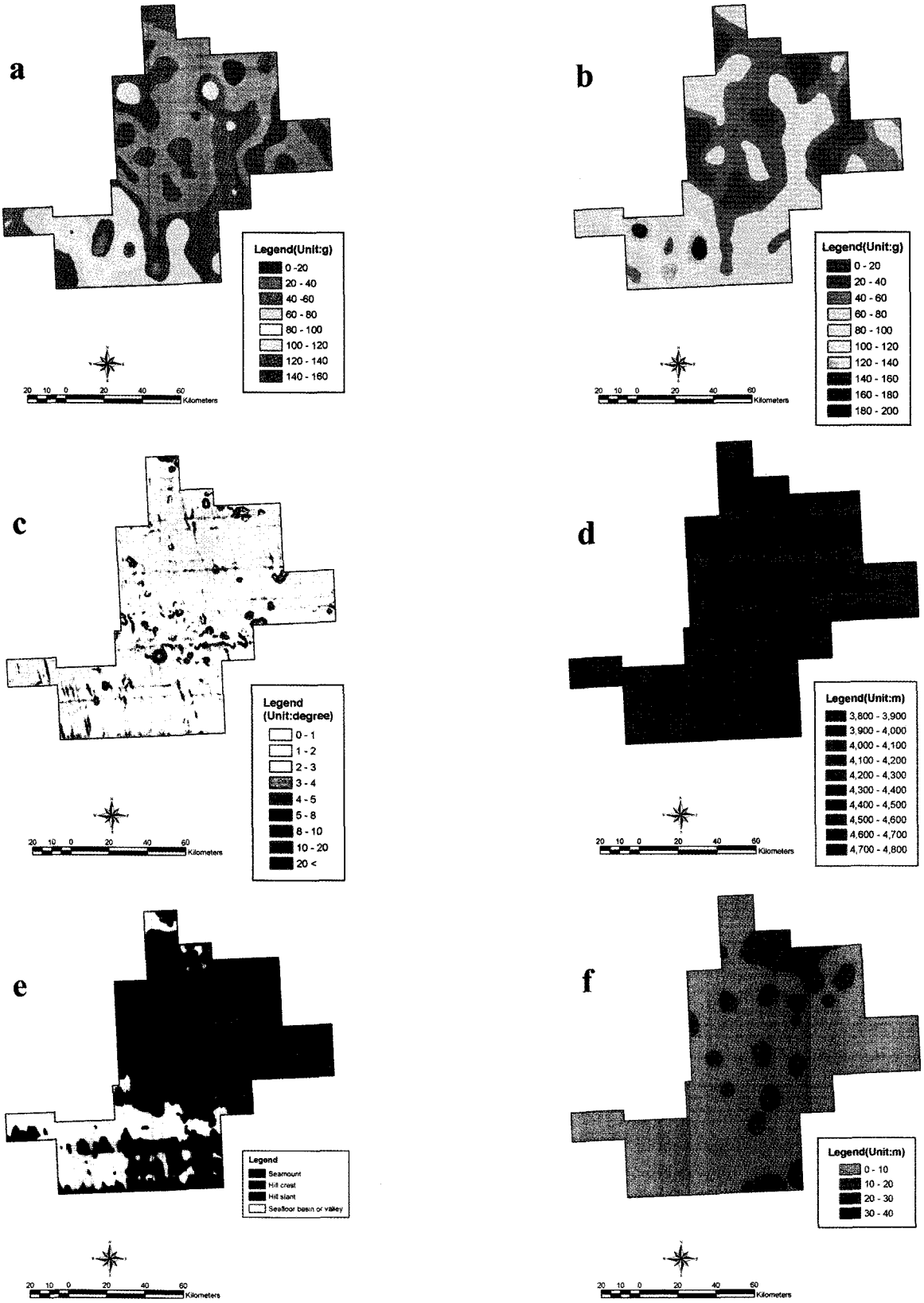

Fig. 5. The distribution map of (a) copper grade, (b) nickel grade, (c) slope, (d) bathymetry, (e) topography, (f) transparent layer thickness, for block N3.

2d). Zones with depths of 4,800 to 5,200 m occupy 88% of the block surface (Fig. 3d). Most sampling stations show water depths between 4,800 and 5,200 m. The water depth increases toward the central part of the block, resulting in a geomorphic trend in a NNW-SSE direction. Rating is highest from 5,000 to 5,200 m interval. In general, the deeper the water depth, the higher the rating.

In block N3, the water depth ranges from 3,852 to 4,709 m with an average of 4,404 ± 108.5 m. Water depth in block N3 is classified into 10 groups (Fig. 4d). Zones with depths of 4,200 to 4,600 m occupy 94% of the block surface (Fig. 5d). Most sampling stations show water depths between 4,200 and 4,600 m interval. The water depth increases toward the west of the block, resulting in a geomorphic trend in a NNW-SSE direction. Rating is highest from 4,500 to 4,700 m interval. In general, the deeper the water depth, the higher the rating.

Relationship between topography and manganese nodule abundance

The topography can be classified into five groups: seamount, hill crest, hill slant, hill base or plain, and seafloor basin or valley. The ratings show lowest value for seamount and hill crest. Ratings generally decrease toward the seafloor basin.

In block N1, seamount zone is defined as topographic high with water depth of 3,632 to 4,500 m. Hill crest zone is defined as topographic high with water depth of 4,500 to 4,700 m. Upper part of the hill that lies between 4,700 and 4,900 m is defined as hill slant zone, and lower part of 4,900 to 5,100 m in depth at the hill base (Fig. 2e). The zone with water depths of 5,100 to 5,485 m is defined as valley. Ratings are high for hill bases and valleys and are low for hill crests and hill slants. Hill slants and hill bases occupied 23%, and 59% of block N1, respectively (Fig. 3e). More than 85% of the sampling stations were located on seamounts, hill slants and plains.

In block N3, seamount zone is defined as topographic high with water depth of 4,394 to 4,500 m. Hill crests are defined as topographic high with water depth of 4,500 to 4,730 m. Upper part of hill that lies between 4,730 and 4,900 m was defined as hill slants, and lower part of hill between 4,900 and 5,000 m in depth is as hill base. The zone with water depth of 5,000 to 5,666 m is defined as valley (Fig. 4e). Hill slants, hell crests and hill bases occupied 72%, and 26% of block N3, respectively. Rating is high for hill bases and valleys, and is low for hill crests and hill slants (Fig. 5e). The seamounts are located in the western and northeastern parts; however, hills are distributed uniformly in block N3.

Relationship between transparent layer thickness and manganese nodule abundance

An inverse relationship between manganese nodule abundance and the thickness of the upper transparent layer can be found in the study area. In block N1, the transparent layer thickness ranged from 0 to 83 m with an average of 11.9±7.0 m (Fig. 2f). The zone with the upper transparent layer thickness 0 to 20 m occupies 90% of block N1. The regression equation obtained using probability methods gives, $Y = -0.54 X + 8.80$, $R^2 = 0.63$. The rating increases for the zone of 0 to 20 m and decreases for the transparent layer above 20 m. Very thick transparent layer is dominant in the southwestern part in block N1 (Fig. 3f).

In block N3, the transparent layer thickness ranges from 0 to 69 m with an average of 28.2 ± 8.2 m. The zone with the upper transparent layer thickness of 15 to 40 m occupies 80% of the surface of block N3. The regression equation obtained using probability methods gives, $Y = -0.57 X + 7.80$, $R^2 = 0.35$. Only a poor correlation between the transparent layer thickness and nodule abundance is found in block N3 (Fig. 4f). The low R^2 value of this block arises from data in class 0 to 5 and anomalous data in class 25 to 30. Without this anomalous data, the R^2 of block N3 increases to 0.73. The occupying zone of class 0 to 5 is 35%; it could be interpreted as a natural phenomenon. The distribution pattern shows a considerable transparent layer thickness along a NW-SE trend in the western part of block N3 (Fig. 5f).

4. Discussion and Conclusion

The greater the copper and nickel grade, the higher the rating. The distribution pattern of nickel grade is similar to that of copper grade. The slopes are generally less than 3°, except for seamounts and cliff areas. There is no increment in the rating with increasing slope. The rating is highest for slopes between 2.5 and 3.5° in block N1 and between 4.0 and 4.5° in block N3. It is difficult to classify topography, because the criterion for topographic classification is not defined clearly in the study area. The ratings prove lowest for seamount and hill crest. It is

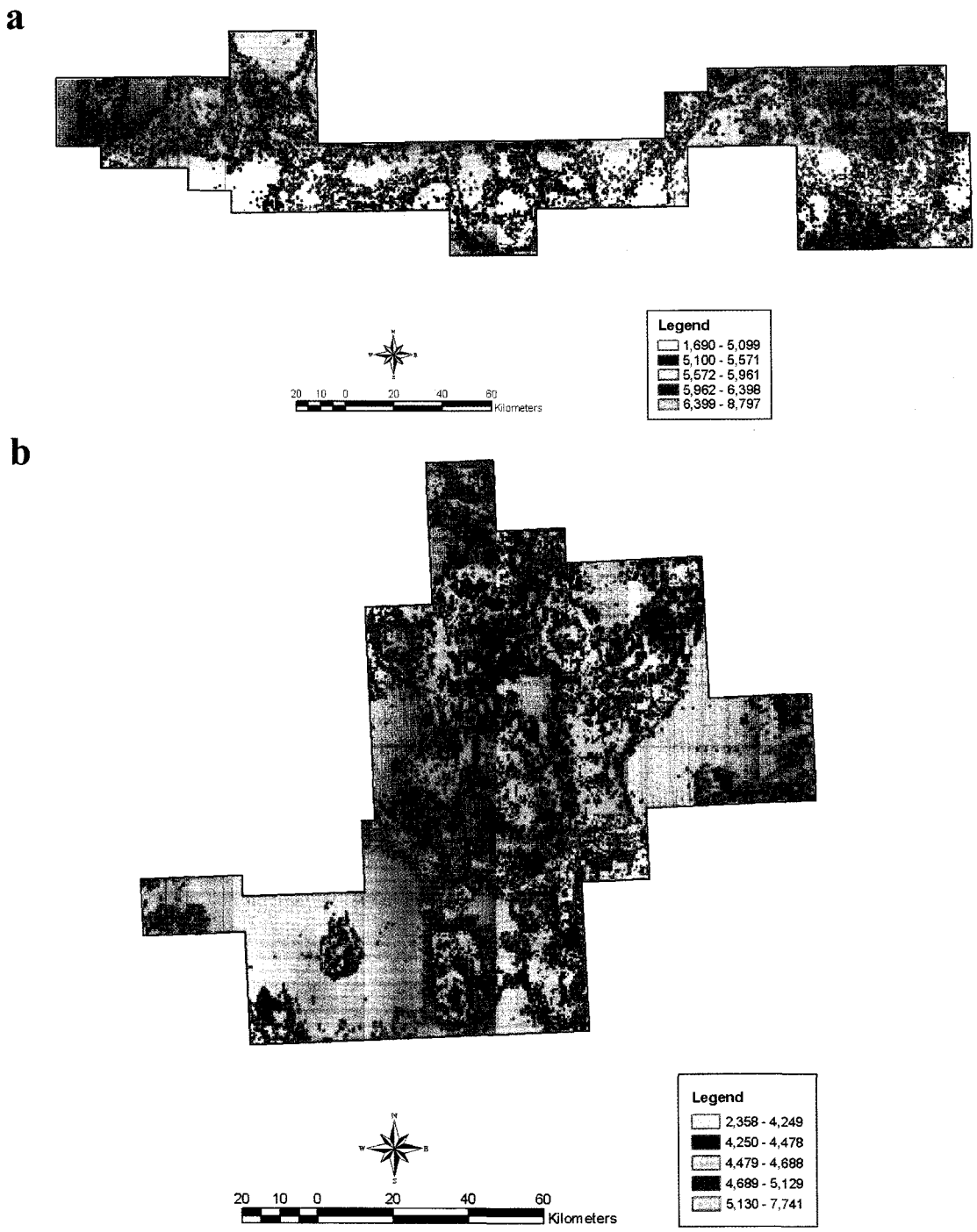

Fig. 6. (a) Nodules development potential index map for block N1, and (b) N3 using GIS. These maps were divided into 10 classes using equal-area method.

difficult to make a precise correlation between seafloor topography and nodule abundance. But as with water depth, the ratings generally increase toward the seafloor basin in the study area. Jeong (1992) proposed that there appeared to be a weak counter-correlation between nodule abundance and water depth in the western part of C-C zone (old Korea Deep Ocean Study area). There is a poor relationship between manganese nodule abundance and the thickness of the upper transparent layer. The difference of R^2 value between N1 and N3 blocks is big. The low R^2

value of block N3 arises from data in class 0 to 5 and anomalous datum in class 25 to 30. When these data are removed, the R^2 of block N3 increases to 0.73. The area occupied by class 0 to 5 is 35%, and it could be interpreted as a natural phenomenon. The rating increases with increasing upper transparent layer thickness to 20 m and decreases over 20 m in block N1, and increases 5 m and decreases over 5 m in block N3.

Six data layers consisting of the applied rating for each parameter, as determined for a specific block and applied to the block itself, were summed to produce a result map called the nodules development potential index map.

The result map was divided into 10 classes using equal-area method. In block N1, two high potential zones are located in the western part with a NE-SW trend, and one high potential area is located in the eastern part with a NW-SE trend. Two high potential areas are located in the central portion with N-S trend (Fig. 6a). In block N3, a rich circular zone occupies the southwestern part, and an impoverished zone the northern part of the block (Fig. 6b).

Acknowledgement

I would like to thank reviewers for their helpful and constructive comments. This work was supported by "The development of deep seabed mineral resources (PM38201 and PM38202)" and "The database construction for seafloor image data by using GIS and the investigation for visualization methods (PE94200)".

References

Allaby A. and M. Allaby. 1999. A Dictionary of Earth Sciences, Oxford University Press. 1999 p.

Archer, A.A. 1976. Prospects for the exploration of manganese nodules: The main technical economic and legal problems. p. 21-38. In: *Papers Presented at the I.D.O.E. Workshop, Suba, Fiji, 1-6 September, 1975*, ed. by G.P. Glasby, and H.R. Katz. Technical Bulletin No.2, U.N. Economic and Social Commission for Asia and the Pacific, CCOP/SOPAC.

Bernhard, H. and H.E. Blissenbach. 1988. Economic importance. p. 4-9. In : *The Manganese nodule belt of the Pacific Ocean*, ed. by P. Halbach, G. Friedrich, and U. von Stackelberg. Ferdinand Enke Verlag, Stuttgart.

Chough, S.K., S.H. Lee, J.W. Kim, S.C. Park, D.G. Yoo, H.S. Han, S.H. Yoon, S.B. Oh, Y.B. Kim, and G.G. Back. 1997. Chirp (2-7 kHz) echo characters in the Ulleung Basin. *Geosci. J.*, **1**, 143-153.

Damuth, J.E. 1978. Echo character of the Norwegian-Greenland Sea: Relationship to Quaternary sedimentation. *Mar. Geol.*, **28**, 1-36.

Damuth, J.E. and D.E. Hayes. 1977. Echo character of the east Brazilian continental margin and its relationship to sedimentary processes. *Mar. Geol.*, **24**, 73-95.

Dowdeswell, J.A., N.H. Kenyon, and J.S. Laberg. 1997. The glacier-influenced Scoresby Sund Fan, East Greenland continental margin: Evidence from GLORIA and 3.5 kHz records. *Mar. Geol.*, **143**, 207-221.

Earney, F.C.F. 1990. Marine Mineral Resources. Routledge. 387 p.

Frazer, J.Z. 1977. Manganese nodule reserves: An update estimate. *Marine Mining*, **1**, 103-123.

Frazer, J.Z. 1979. The reliability of available data on element concentrations in seafloor manganese nodules. In: *Manganese Nodules Dimensions and Perspective*. Dordrecht Reidel.

Glasby, G.P. 1978. Deep-sea manganese nodules in the stratigraphic record: Evidence from DSDP cores. *Mar. Geol.*, **28**, 51-64.

Holser, A.F. 1976. Manganese nodule resources and mine site availability (Professional staff study, ocean mining Administration, Department of Interior, Washington, D.C.). (Unpublished)

IFREMER, 1989. Evaluation et étude des moyens necessaires à l'exploitation des nodules polymetalliques. Rapport final, TOME I, pp. 1/1-5/10. (Unpublished)

Japan International Cooperation Agency, Metal Mining Agency of Japan. 2000. Report on the cooperative study project on the deep sea mineral resources in selected offshore areas of the SOPAC region; Data analysis and digitalization between 1985 and 2000. 354 p. (Unpublished)

Jeong, K.S., J.K. Kang, K.L. Lee, H.S. Jung, S.B. Chi, and S.J. Ahn. 1996. Formation and distribution of manganese nodule deposit in the northwestern margin of Clarion-Clipperton fracture zone, northeast equatorial Pacific. *Geo-Marine Lett.*, **16**, 123-131.

Jeong, K.S., J.K. Kang, and S.K. Chough. 1994. Sedimentary process and manganese nodule formation in the Korea Deep Ocean Study (KODOS) area, western part of Clarion-Clipperton fracture zones, northeast equatorial Pacific. *Mar. Geol.*, **122**, 125-150.

Jones, E.J.W. 1999. Marine Geophysics. John Wiley & Sons. 466 p.

Jung, H.S. and C.B. Lee. 1999. Growth of diagenetic ferromanganese nodules in an oxic deep-sea sedimentary environment, NE equatorial Pacific. *Mar. Geol.*, **157**, 127-144.

Kildow, J.T., M.B. Bever, V.K. Dar, and A.E. Capstaff. 1976. Assessment of economic and regulatory conditions affecting ocean minerals resources department (Report to the Department of Interior, Massachusetts Institute of Technology, Cambridge). (Unpublished)

Kim, H. S., T.G. Lee, Y.T. Ko, and K.H. Kim. 1998. Relationship

between manganese nodule occurrence and the acoustically-transparent uppermost sedimentary layer in the Korea Deep Ocean Study (KODOS) 98-1 area, northeast equatorial Pacific. *Ocean Res.*, **20**(3), 275-284.

Ko, Y.T. 1997. A suitable site selection study for manganese nodules development by using GIS in northeastern pacific KODOS area. M.S. Thesis. Yonsei University, Korea.

Kuhn, G. and M.E. Weber. 1993. Acoustical characterization of sediments by Parasound and 3.5 kHz systems: Related sedimentary processes on the southeastern Weddell Sea continental slope, Antarctica. *Mar. Geol.*, **113**, 201-217.

Manheim, F.T. 1978. Book review of G. P. Glasby, Marine Manganese Deposits. *Geochemica et Cosmochimica Acta*, **42**(5), 541.

MOMAF. 1996. A report on '96 deep seabed mineral resources exploration. MOMAF, Seoul. 954 p.

MOMAF. 1997. A report on '97 deep seabed mineral resources exploration. MOMAF, Seoul. 843 p.

MOMAF. 1999. A report on '99 deep seabed mineral resources exploration. MOMAF, Seoul. 780 p.

Mckelvey, V.E., N.A. Wright, and R.W. Rowland. 1979. Manganese nodule resource in the northeastern equatorial Pacific. p. 747-762. In: *Marine Geology and Oceanography of the Pacific Manganese Nodule Province*, ed. by J.L. Bischoff and D. Z. Piper. Plenum, New York.

Medwin, H. and C.S. Clay. 1997. Fundamentals of acoustical oceanography. Academic Press. 712 p.

Mero, J.L. 1965. The mineral resources of the sea. Elsvier, Amsterdam. 312 p.

Mizuno, A., T. Miyazaki, A. Nishimura, K. Tamaki, and M. Tanahashi. 1980. Central Pacific manganese nodules, and their relation to sedimentary history. *Offshore Tech. Conf.*, **3830**, 331-340.

OMCO. 1992. Methods for correcting nodule abundance estimates based upon free-fall grab recoveries. Exploration data transfer between Ocean Minerals Company and Korea Ocean Research and Development Institute. 450 p.

Park, C.Y. 1995. A geostatistical study on reserve estimation of manganese nodule deposits in Korea Deep Ocean Study (KODOS) area. Ph. D. Thesis. Seoul National University, Korea. 160 p.

Pratson, L.F. and E.P. Laine. 1989. The relative importance of gravity-induced versus current-controlled sedimentation during the Quaternary along the mideast United-States outer continental margin revealed by 3.5 kHz echo character. *Mar. Geol.*, **89**, 87-126.

Skornyakova, N.S. and I.O. Murdmaa. 1992. Local variation in distribution and composition of ferromangansese nodules in the Clarion-Clipperton nodule province. *Mar. Geol.*, **103**, 381-405.

Taylor, J., J.A. Dowdeswell, N.H. Kenyon, R.J. Whittington, T.C.E. van Veering, and J. Mienert. 2000. Morphology and Late Quaternary sedimentation on the North Faeroes slope and abyssal plain, North Atlantic. *Mar. Geol.*, **168**, 1-24.

Usui, A., A. Nishimura, M. Tanahashi, and S. Terashima. 1987. Local variation of manganese nodule facies on small abyssal hills of the Central Pacific Basin. *Mar. Geol.*, **74**, 237-275.

Usui, A. and M. Tanahashi. 1986. Relationship between local variation of nodule facies and acoustic stratigraphy in the GH81-4 area. *Geol. Surv. Japan Cruise Rept.*, **21**, 160-170.

Usui, A. and M. Tanahashi. 1992. Relationship between local variation of nodule facies and acoustic stratigraphy in the Southern part of the Central Pacific Basin (GH82-4 area) *Geol. Surv. Japan Cruise Rept.*, **22**, 219-231.

von Stackelberg, U. and H. Beiersdorf. 1991. The formation of manganese nodules between the Clarion and Clipperton fracture zones southeast of Hawaii. *Mar. Geol.*, **98**, 411-423.